

Damage pattern, bedrock geology and surface ruptures of the 2009 L'Aquila event and implications for seismic hazard planning

I. Papanikolaou

Laboratory of Mineralogy & Geology, Department of Geological Sciences and Atmospheric Environment, Agricultural University of Athens, Athens, Greece
AON Benfield Hazard Research Centre, Department of Earth Sciences Birkbeck College and University College London, London, UK

E. Lekkas & I. Fountoulis

Department of Dynamic, Tectonic and Applied Geology, National and Kapodistrian University of Athens, Athens, Greece

Is. Parcharidis

Department of Geography, Harokopio University of Athens, Athens, Greece

M. Fomelis

Department of Geophysics—Geothermics, National and Kapodistrian University of Athens, Athens, Greece

ABSTRACT: This paper examines how the damage pattern of the 2009 $M_w = 6.3$ L'Aquila event correlates: a) with the bedrock geology, b) the amount of uplift/subsidence values recorded by the DInSAR analysis and c) the fault geometry. Moreover, it examines the widespread primary and secondary surface ruptures and the implications for the seismic hazard assessment for planning and design purposes. The amount of the DInSAR recorded uplift or subsidence values do not correlate to the damage pattern, implying that bedrock geology is the predominant factor that explicitly overshadows all other effects.

1 INTRODUCTION

The 2009 $M_w = 6.3$ L'Aquila earthquake in central Italy despite its moderate magnitude caused significant loss of life (~300 fatalities) and damages, producing the highest death toll in the European Union since the 1980 $M_w = 6.9$ Irpinia event and the highest economic cost since the 1999 $M_s = 5.9$ Athens earthquake. Such moderate events have a high rate of occurrence and due to their proximity to human habitation, pose a high risk in most extensional settings, forming a typical case study scenario. This event offered a plethora of information that is useful for seismic hazard assessment and planning. In this paper we focus our attention: a) on the primary and secondary surface ruptures (where they have been occurred and whether they could have been predicted), b) on the damage pattern and how it correlates both with the bedrock geology and the uplift/subsidence values recorded by the DInSAR analysis.

2 THE 2009 $M_W = 6.3$ EARTHQUAKE IN L'AQUILA

The earthquake based on body wave seismology, InSAR, and GPS data was assessed as a $M_w = 6.3$, at a focal depth of 9 km, having a normal faulting mechanism of $N147^\circ$ striking and dipping at $\sim 50^\circ$ towards the SW with a maximum $\sim 0.6\text{--}0.9$ m slip (Walters et al. 2009,

Atzori et al. 2009, Chiarabba et al. 2009). The macroseismic epicentre was the village of Onna (MCS intensity IX-X) located about 12 km east from the earthquake epicentre, whereas the town of L'Aquila suffered intensity VIII-IX (Quest 2009).

3 GEOLOGICAL SETTING AND ACTIVE FAULTS

The earthquake occurred on one of the NW-SE trending normal faults that form part of the 800 km long segmented normal fault system (Fig. 1a) that accommodates extension in the Apennines (e.g. Anderson and Jackson 1987, Roberts et al. 2002). These faults tend to generate strong events from $M = 5.5$ up to $M = 7.0$ and depending on the magnitude and the earthquake depth can produce from minor to severe damages and occasionally destruction (Michetti et al. 1996, Galadini and Galli 2000, Roberts et al. 2004). The town of L'Aquila is not only surrounded by several active normal faults, but is situated on their hangingwall as well (Fig. 1b). Each major fault comprises of several overlapping segments, closely spaced parallel segments and even antithetic structures. These antithetic structures are all high angle normal faults and closely spaced (~3–4 km) with the main faults, so that in most cases are linked at depth. This is the case of the L'Aquila fault that creates a complex fault structure, often leading to different interpretations.

The L'Aquila fault is a 37 km long structure that strikes northwest-southeast and down-throws to the southwest (Roberts and Michetti 2004). This fault has a rather complex structure, since it comprises several overlapping segments some of which are antithetic to the main SW dipping fault plane (Papanikolaou et al. 2005). These antithetic planes are nicely observed northwards the village of Barisciano, have fresh looking fault planes and are probably kinematically linked to the NE dipping Bazzano—Fossa fault segments in the southern part of the valley. The Mt Pettino, the Paganica segment (or Aquilano fault Boncio et al. 2004) and the antithetic Bazzano—Fossa fault outcrop on either side of the valley (Michetti et al. 2000) and form part of the same system. In a few words the strain in the area is accommodated on multiple closely spaced synthetic and antithetic overlapping segments. Therefore, the fault zone is characterised by distributed displacement on several overlapping faults that break up the footwall and the hanging wall into smaller blocks. This earthquake has activated one of the fault segments of the L'Aquila fault that bounds the northern part of the Aterno valley in Paganica (Fig. 1b, Michetti et al. 2009).

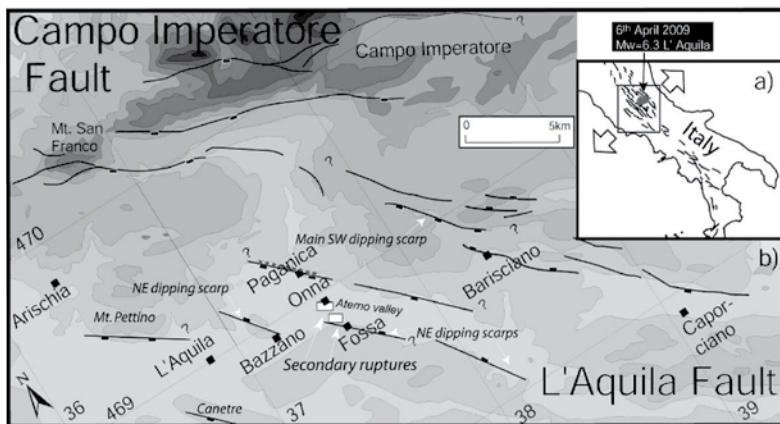


Figure 1. Map of the Italian Peninsula showing the active faults, the NE-SW extension occurring in Abruzzo and the epicenter of the 6th of April 2009 $M_w = 6.3$ event (Roberts et al. 2002). b) Detailed topographic map in L'Aquila showing the fault segments and the primary surface ruptures with red dashed line (modified from Michetti et al. 2000, Roberts and Michetti 2004, Papanikolaou et al. 2005).

4 PRIMARY AND SECONDARY SURFACE RUPTURES

This earthquake despite its moderate magnitude produced a plethora of Earthquake Environment Effects involving primary and secondary surface ruptures, rockfalls, landslides and liquefaction phenomena, covering an area of almost 1,000 km² (Blumetti et al. 2009). Surface ruptures, in particular, were widespread and of significant importance. These ruptures were all NW-SE trending parallel to the activated fault plane and have throws ranging from a few cm up to a couple of tens of cm (e.g. Blumetti et al. 2009, DST Working Group—Uni CHB 2009, INGV-Emergeo Group 2009, Michetti et al. 2009). Three main rupture categories have been distinguished.

4.1 *Primary surface ruptures*

Primary surface ruptures represent the surface expression of the activated seismogenic fault. They were discontinuous, but well aligned and could be traced up for at least 2.6 km with maximum displacements not exceeding 10 cm in Paganica (Michetti et al. 2009, Fig. 2). Due to the moderate magnitude of this earthquake, primary surface ruptures had small displacements that did not exceed 10–12 cm, implying that it was difficult to distinguish between primary and secondary ruptures. However, all researchers agree that the surface ruptures traced in Paganica were primary and this occurs not only because they correlate well with the focal mechanism and the epicenter locality, but also due to the DInSAR analysis that provides a clear view of the surficial deformation pattern (see also Section 6). The DInSAR predicted fault surface ruptures coincide with the ground surface ruptures observed in Paganica, confirming that the ruptures observed near Paganica were indeed primary. Additionally, these ruptures broke a 0.7 m diameter high pressure water pipeline in Paganica.

4.2 *Secondary surface ruptures on pre-existing fault planes*

Several secondary surface ruptures occurred on neighboring pre-existing fault planes. Several reports describe such ruptures in the Roio—Canetre fault, the NE dipping Bazzano fault, where a 5–8 cm white stripe at the base of the limestone fault scarps was observed (Fig. 2) and locally on the Mt. Pettino segment and the Campo Imperatore fault (Blumetti et al. 2009, DST Working Group—Uni CHB 2009, INGV-Emergeo Group 2009, Michetti et al. 2009).

4.3 *Secondary surface ruptures on recent unconsolidated sediments within the Aterno valley*

Tens of secondary surface ruptures were widespread within the recent sediments of the Aterno basin, reaching up to several tens of meters long (Fig. 3). They are highly correlated with the damage pattern since the majority of them occurred near the village of Onna that suffered the highest damages. These secondary ruptures are several tens of meters long and up to 30 cm wide and are all strictly NW-SE trending parallel ($150^\circ \pm 20^\circ$) to the activated fault plane. They are mostly observed near the river as well as on manmade road embankments (Fig. 3). Overall, these



Figure 2. Views of the primary surface ruptures in Paganica (left) and the secondary surface ruptures in the Bazzano fault (right) (courtesy E. Vittori).



Figure 3. View of the secondary ruptures near the village of Onna.

secondary ruptures appeared in artificial and natural structures that are prone to rupturing. Most of these ruptures were transverse to the road network, producing cracks in paved roads that are several meters long and having offsets both horizontal and vertical of several cm (up to 6 cm).

These secondary surface ruptures can cause significant damage, but they are usually disregarded in seismic hazard assessment studies for planning and design purposes. This earthquake also showed that existing fault planes even if they have not been activated may experience secondary ruptures. Therefore, faults not only form preferential travel pathways for the seismic waves, thus enhancing the seismic shaking, but may experience secondary ruptures as well. The latter increase their potential hazard to an upper level that should be considered as well. Even if these types of ruptures that occur on pre-existing fault planes can be predicted, several others that occur on recent unconsolidated sediments can not. They tend to occur on manmade embankments and natural structures prone to rupturing, indicating that all constructions are highly vulnerable in such settings. As a result, it is important to consider possible dislocations for planning and design purposes of critical facilities with displacements ranging from several cm up to a few decimeters both in areas considered susceptible for such secondary ruptures as well as on pre-existing active or even inactive fault planes.

5 MACROSEISMIC INTENSITIES, FAULT GEOMETRY AND BEDROCK GEOLOGY

The macroseismic epicentre was the village of Onna (MCS intensity IX-X) that suffered the highest damages and recorded the highest death toll (losing 10% of its population), located about 12 km east from the earthquake epicentre, whereas the town of L'Aquila suffered intensity VIII-IX (Quest 2009). In Figure 4, the MCS intensity values assessed from the Quest team, have been superimposed on the official 1:50.000 scale geological map of the area.

Despite the fact that the fault plane ruptured up to the surface near the Paganica village, it is interesting to note that the Paganica village suffered moderate damage (VIII). Several other neighboring villages in the immediate footwall of the ruptured plane, such as Pescomaggiore, Petogna and San Martino, experienced minor to moderate damages (VI up to VII-VIII). On the other hand, villages located within the Aterno Basin in the hanging wall, suffered significant damages (Onna IX-X, San Gregorio IX, Villa Sant'Angelo IX, Sant' Eusanio Forconese IX). The majority of the damages in these villages relate to old masonry buildings (Fig. 5). Overall, the damage pattern is elongated along a NW-SE direction, which reflects the activated fault plane, the elongated geological structure of the recent sediments of the Aterno valley and involves also some directivity effects. The damage pattern varies over short distances due to changes in bedrock geology. The most striking example involves the villages of Onna and Monticchio that are only 1.5 km apart, but their MCS recordings differ up to 3.5 intensity values. The Monticchio village is founded on bedrock (limestones) and recorded intensity VI, whereas the village of Onna is founded on recent alluvial sediments underlain by 100 m of lacustrine sediments and recorded intensity IX-X (Fig. 4).

The L'Aquila basin is characterised by unfavourable site specific conditions since it is filled with a few hundred meters of lacustrine sediments that overlie the bedrock (Blumetti et al.

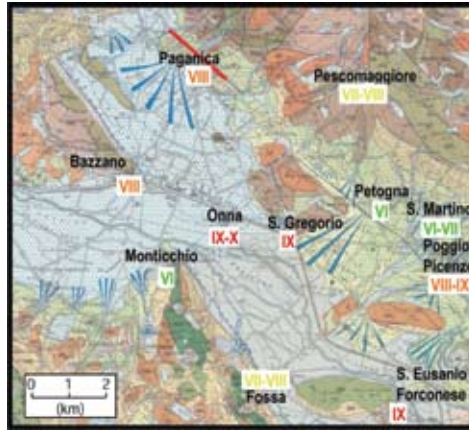


Figure 4. View of the official geological map (CARG N. 359 L'Aquila) in the epicentral area. Superimposed are the primary surface ruptures and the intensities recorded by the Quest 2009 team. Intensities are highly influenced by the bedrock geology.



Figure 5. View of the extended damages and collapses towards the village of Onna.

2002). This produces significant ground motion amplification at low frequencies (~ 0.6 Hz) as has been demonstrated by De Luca et al. (2005) using weak motion and ambient noise data. This amplification is mostly attributed to the couple of hundred meters thick lacustrine sediments.

6 THE DINSAR INPUT AND THE DEFORMATION PATTERN

The Differential Radar Interferometry (DInSAR) technique has been used to detect surface displacements in the order of a few centimetres. This technique combines and merges two radar images acquired before and after the earthquake in order to trace the differences caused by the earthquake, offering a detailed view of the deformation pattern. Figure 6 shows the differential interferogram, whose pattern is asymmetrical since the deformed area is significantly expanded to the southeast. The deformed area is about 460 km², of which 66% (or 305 km²) has subsided and the remaining 34% (or 155 km²) has been uplifted (Papanikolaou et al. 2010). The maximum observed uplift was about 10 cm and was recorded a couple of km northeast from the Paganica surface ruptures in the immediate footwall of the fault, whereas the maximum subsidence was 25 cm and was observed about 2 km SW from the NE dipping Bazzano fault. A cross section drawn across strike of the activated fault plane, showing the uplifted and subsided area, allows the fault trace to be easily traced with high precision (Fig. 6). The DInSAR predicted fault surface ruptures coincide with localities where surface ruptures have been observed in the field, confirming that the ruptures observed near Paganica are indeed primary. This is an important outcome because this earthquake as demonstrated previously produced both primary and secondary ruptures of similar displacements, many of which occurred on pre-existing fault planes. The latter implies that it was

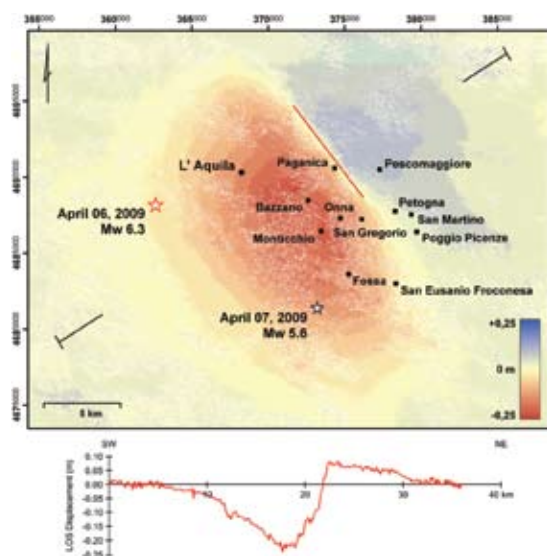


Figure 6. View of the DInSAR deformation field and the predicted primary fault surface rupture locations. Cross section is across strike of the activated fault plane and shows the uplift and subsidence in the footwall and hanging wall.

difficult to distinguish between primary ruptures that are the expression of the activated fault plane in the surface and secondary ruptures which are triggered by the earthquake and correspond mostly to gravitational effects, without the DInSAR input.

7 CORRELATING DINSAR DISPLACEMENT VALUES AND THE DAMAGE PATTERN

We tried to test whether the amount of uplift or subsidence that each locality experienced (Fig. 6) is correlated to the damage pattern (Fig. 4). Displacement values were extracted from the DInSAR and correlated to the macroseismic intensity values MCS (Quest 2009). Table 1 displays the displacement and intensity values and Figure 7 shows that there is no correlation between the recorded amount of uplift or subsidence values and the macroseismic intensity.

The majority of the damages in these villages relate to old masonry buildings so that the building stocks are of the same construction quality. There is no correlation even if uplift or subsidence values are examined separately. It is interesting to note that the village of Paganica in the immediate hanging wall of the activated fault, where the primary surface ruptures were recorded, was subsided for only 6.4 cm and experienced intensity VIII. On the other hand, the village of Onna that was the macroseismic epicenter experienced intensity IX-X and subsidence of 17 cm, whereas the village of Monticchio that was only 1.5 km away from the village of Onna and 4 km away from the primary surface ruptures, subsided 20.5 cm but experienced macroseismic intensity of only VI.

It is evident that villages that recorded uplift are characterized by lower damages. This is expected because damages on the footwall are usually lower, since secondary effects are fewer and in most cases bedrock is exposed on footwall. Moreover, the villages of Poggio Picenze and San Eusanio Froconesa that recorded negligible values of displacement (1 cm of uplift and 3 cm of subsidence respectively) experienced severe damages (IX intensity). This is probably because they are both on the prolongation of the activated fault plane and the rupture propagation and thus suffered from the strong SE oriented directivity effects as the PGA values explicitly shows (e.g. Ameri et al. 2009, Akinci et al. 2010). Therefore, it is highly interesting that the amount of the DiNSAR recorded uplift or subsidence values do

Table 1. DInSAR Displacement in cm and intensity values (Quest 2009) in the epicentral area.

LOCALITY	DInSAR (cm)	Mercalli (MCS)
Paganica	-6.5	VIII
Pescomaggiore	+6.4	VII-VIII
Bazzano	-18.7	VIII
Onna	-17.0	IX-X
Monticchio	-20.6	VI
San Gregorio	-10.4	IX
Fossa	-14.6	VII-VIII
Petogna	+1.4	VI
San Martino	+2.2	VI-VII
Poggio Licenze	+1.2	VIII-IX
S. Eusanio Froconesa	-2.0	IX

Positive values (+) correspond to uplift.
 Negative values (-) to subsidence.

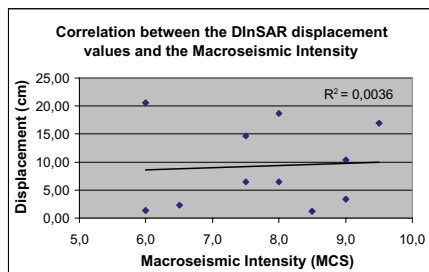


Figure 7. Diagram showing that there is no correlation between the amount of uplift or subsidence and the intensity values.

not correlate to the damage pattern, implying that bedrock geology is the predominant factor that explicitly overshadows all other effects in this earthquake.

8 CONCLUSIONS

The main outcomes can be summarized in the following paragraphs:

- The large number and extensive spatial distribution of secondary surface ruptures that occurred not only within the recent sediments of the Aterno basin, but also on pre-existing fault planes was a major feature of this earthquake. These ruptures are usually disregarded in seismic hazard assessment planning and design studies, but can produce significant damage. Their throw exceeded several cm, a value which is significantly higher than the expected compaction subsidence values in sediments. As a result, it is important to consider possible dislocations with displacements ranging from several cm up to a few decimeters both in areas considered susceptible for such secondary ruptures as well as on pre-existing active or even inactive fault planes. A maximum dislocation value that will not exceed 20 cm of displacement in similar geological settings should be established to relevant susceptible sites for planning and design purposes of critical facilities such as major pipeline routes.
- The interferogram offered a valuable input in this earthquake, providing a clear view of the surficial deformation pattern. The DInSAR predicted fault surface ruptures coincide with localities where surface ruptures have been observed in the field, confirming that the ruptures observed near Paganica are indeed primary, whereas all others were secondary.
- Fault geometry influenced significantly the damage pattern. Villages located on the hanging wall experienced higher intensity values, compared to villages located on the footwall. This is also verified by the DInSAR which shows that the hanging wall area was subjected to higher deformation values. On average, subsidence values were two and a half times larger than the uplift values and correlated with more violent shaking.
- Basin effects and the bedrock geology played once more a decisive role to the damage pattern, even at short distances. Villages that were only 1.5 km apart, recorded up to 3.5 intensity values difference. In particular, the Monticchio village founded on bedrock recorded intensity VI, whereas the village of Onna founded on recent alluvial sediments overlying one hundred meters of lacustrine sediments recorded intensity IX-X.
- The amount of the DInSAR recorded uplift or subsidence does not correlate with the intensity of shaking, implying that bedrock geology is the predominant factor that governs the damage pattern and explicitly overshadows all other effects in this earthquake.

REFERENCES

- Anderson, H. and Jackson, J. (1987). Active tectonics of the Adriatic region. *Geophysical Journal of the Royal Astronomical Society* 91, 937–983.
- Akinci, A., Malagnini, L. and Sabetta, F. (2010). Characteristics of the strong ground motions from the 6 April 2009 L'Aquila earthquake, Italy. *Soil Dynamics and Earthquake Engineering* 30, 320–335.
- Ameri, G., et al. (2009). The 6 April 2009 Mw 6.3 L'Aquila (Central Italy) Earthquake: Strong-motion Observations. *Seismological Research Letters* 80, 951–966.
- Atzori, S., et al. (2009). Finite fault inversion of DInSAR coseismic displacement of the 2009 L'Aquila earthquake (central Italy). *Geophys. Res. Lett.* 36, L15305, doi:10.1029/2009GL039293.
- Blumetti, A.M., et al. (2009). Gli effetti ambientali della sequenza sismica dell' Aprile 2009 in Abruzzo. Il terremoto Aquilano dell' aprile 2009: primi risultati e strategie future, Chieti.
- Blumetti, A.M., Di Filippo, M., Zaffiro, P., Marsan, P. and Toro, B. (2002). Seismic hazard of the city of L'Aquila (Abruzzo-Central Italy): new data from geological, morphotectonic and gravity prospecting analysis. *Studi Geologici Camerti* 1, 7–18.
- Boncio, P., Lavecchia, G. and Pace, B. (2004). Defining a model of 3D seismogenic sources for seismic hazard assessment applications: The case of central Apennines (Italy). *J. Seism.* 8, 407–423.
- Chiarabba, C., et al. (2009). The 2009 L'Aquila (central Italy) Mw 6.3 earthquake: Main shock and aftershocks. *Geophys. Res. Lett.* 36, L18308, doi:10.1029/2009GL039627.
- De Luca, G., Marcucci, S., Milana, G. and Sano, T. (2005). Evidence of Low-Frequency amplification in the City of L'Aquila, Central Italy, including strong and weak motion data, ambient noise and numerical modelling. *Bull. Seism. Soc. America* 95, 1469–1481.
- DST Working Group-Uni Ch, (2009). The L'Aquila earthquake of April 2009 seismotectonic framework and coseismic ground features. Edts Boncio, P. Lavecchia, G. & Pizzi, A. 7 p.
- Galadini, F. and Galli, P. (2000). Active tectonics in the Central Apennines (Italy) - Input Data for Seismic Hazard Assessment. *Natural Hazards* 22, 225–270.
- INGV-Emergeo working group (2009). Rilievi geologici di terreno effettuati nell'area epicentrale della sequenza sismica dell' Aquilano del 6 aprile 2009. *Quaderni di Geophysica* 70, 1–53.
- Michetti, A.M., et al. (2009). Earthquake ground effects during moderate events: The L'Aquila 2009 event case history. 1st INQUA-IGCP-567 International Workshop on Earthquake Archeology and Palaeoseismology, 87–90.
- Michetti, A.M., Brunamonte, F., Serva, L. and Vittori, E. (1996). Trench investigations of the 1915 Fucino earthquake fault scarps (Abruzzo, Central Italy): geological evidence of large historical events. *Journal of Geophysical Research* 101, 5921–5936.
- Michetti, A.M., Serva, L. and Vittori, E. (2000). ITHACA, a database of active capable faults of the Italian onshore territory. Report of ANPA-Agenzia Nazionale Protezione Ambiente, Rome.
- Papanikolaou, I.D., Fomelis, M., Parcharidis, I., Lekkas, E.L. and Fountoulis, I.G. (2010). Deformation pattern of the 6 and 7 April 2009, Mw = 6.3 and Mw = 5.6 earthquakes in L'Aquila (Italy) revealed by ground and space based observations. *Nat. Hazards Earth Syst. Sci.* 10, 73–87.
- Papanikolaou, I.D., Roberts, G.P. and Michetti, A.M. (2005). Fault scarps and deformation rates in Lazio-Abruzzo, Central Italy: Comparison between geological fault slip-rate and GPS data. *Tectonophysics* 408, 147–176.
- QUEST 2009. Quick Earthquake Survey Team, Civil Protection Department and INGV. Rapporto sugli effetti del terremoto aquilano del 6 aprile 2009. Rapporto congiunto DPC-INGV Galli, P. and Camassi, R. (eds.) (<http://www.mi.ingv.it/eq/090406/quest.html>.)
- Roberts, G.P., Cowie, P., Papanikolaou, I. and Michetti, A.M. (2004). Fault scaling relationships, deformation rates and seismic hazards: An example from the Lazio-Abruzzo Apennines, central Italy. *J. Struct. Geol.* 26, 377–398.
- Roberts, G.P. and Michetti, A.M. (2004). Spatial and temporal variations in growth rates along active normal fault systems: an example from the Lazio-Abruzzo, central Italy. *J. Struct. Geol.* 26, 339–376.
- Roberts, G.P., Michetti, A.M., Cowie, P., Morewood, N.C. and Papanikolaou, I. (2002). Fault slip-rate variations during crustal-scale strain localisation, central Italy. *Geophys Res. Lett.* 29, 10.1029/2001GL013529.
- Servizio Geologico d' Italia (2006). Cartografia geologica ufficiale Foglio 1:50.000 N. 359, L'Aquila.
- Walters, R.J., et al. (2009). The 2009 L'Aquila earthquake (central Italy): A source mechanism and implications for seismic hazard. *Geophys. Res. Lett* 36, L17312, doi:10.1029/2009GL039337.